Shielding and Radiation Characteristics of Cylindrical Layered Bianisotropic Structures

Lucio VEGNI, Alessandro TOSCANO

Dept. of Applied Electronics, University "Roma Tre", via della Vasca Navale, 84 00146 Rome, Italy

vegni@uniroma3.it, toscano@ieee.org

Abstract. *In this paper we propose an analytical study in the spectral domain of cylindrical layered structures filled with general bianisotropic media and fed by a 3D electric source. The integrated structure is characterized in terms of transmission matrices leading to an equivalent circuit representation of the whole multilayered structure. Within the framework of this two-port formalism, we present a new contribution to the computation of the Green's function arising in the analysis of multilayered conformal integrated antennas loaded with general bianisotropic materials. We also propose an analytical study of the shielding effectiveness of general bianisotropic materials located in multilayered, cylindrical configuration. The expression of the shielded fields sustained both by plane wave and arbitrary sources is obtained in a closed analytical form. Numerical results are also presented showing effects of electromagnetic parameters on radiation pattern, matching properties and radar cross section of the integrated structure.*

Keywords

Cylindrical antennas, bianisotropic media, dyadic Green's functions, shielding.

1. Introduction

The explosion of personal communications and the perspectives of a large expansion in space and terrestrial multimedia, as well as microwave sensing and localization services, have introduced new requirements:

- Extensive re-use of frequency resources in complex propagation environments,
- Multiple beam operation with low side lobes for interference control,
- Miniaturization, low cost and/or conformal design.

These requirements can only be met with innovative or smart antennas in their broad sense. Modern answer to this problem are conformal antennas, extremely thin antennas which are embedded or mounted on curved structures.

In the last years, in fact, much attention has been paid to the design of high-performance antennas. Accurate control of radiation properties is very important in electromagnetic engineering applications. To this end there is a need to develop analytical and numerical techniques able to predict in detail the radiation and scattering performance of microstrip patch antennas on planar and curved surfaces.

On the other hand, the interaction of the electromagnetic field at microwave frequencies with layered bianisotropic media has attracted the attention of the electromagnetic community due to its potential applications in the field of antennas, microwave devices etc. [1]–[3].

Conformal antennas have been analyzed using a number of different techniques. The techniques used in these papers include Finite Element Method (FEM) [4], [5], Method of Moments (MoM) [6]. In the past, the geometrical theory of diffraction (GTD) was also successfully applied to predict the changes in the radiation pattern of the aperture antennas caused by a finite ground plane [7]–[8].

The FEM has a relatively simple formulation and is attractive for complex, relatively small structures. Also, it results in sparse, banded matrices that can be effectively stored and solved. However, the FEM when used alone does not incorporate the Sommerfeld radiation condition and hence requires discretization to extend far from the source region so that the radiation condition can be imposed. Recent efforts have concentrated on the use of absorbing boundary conditions to reduce the discretization region [9]. Unfortunately, the accuracy of these approximate boundary conditions depends on specific problem geometry, leading to results of unpredictable accuracy. The method of moments (MoM), on the other hand, incorporates the Sommerfeld radiation condition through the use of the appropriate Green's function. As a result, the domain discretization can be kept to a minimum. However, this method has the disadvantage of being difficult to implement for complex penetrable structures. This method also results in dense matrices whose treatment requires a big storage.

This paper deals with the analysis of circular cylindrical multilayered structures loaded with bianisotropic and/or inhomogeneous dielectric slabs in presence of microstrip patches for conformal arrays through the integral equation (IE) formulation combined with the method of moment (MoM) algorithms. To eliminate the disadvantages of this method, we propose a combined approach based on a generalization of the Immittance Matrix Approach and the Method of Line in the spectral domain.

First, the Maxwell's equations will be rewritten in terms of a coupled transmission line circuit equivalent representation for linear, homogeneous, bianisotropic circular cylindrical media. Second, the Shielding Effectiveness will be written in a closed analytical form, in terms of the primary constants of the transmission line circuit equivalent representation obtained.

The numerical method used is the method of moments in combination with a radial expansion scheme. Input impedance, mutual coupling and shielding effectiveness are calculated and results are validated against measurements on an experimental model.

2. Formulation of the Electromagnetic Problem

2.1 Spectral Transmission-Line Equations

The extension of the Immittance Matrix Approach proposed in [10–16] for the computation of the fields produced by three-dimensional (3D) sources embedded in a general stratified medium with circular cylindrical symmetry filled with general bianisotropic media creates some difficulties since this method was originally developed to deal only with planar stratified structures with isotropic layers. We start from the Maxwell's equations ($e^{j\omega t}$ time dependence is assumed) for general bianisotropic media:

$$\begin{cases} \nabla\times\mathbf{E} = -j\omega\underline{\boldsymbol{\tau}}\bullet\mathbf{E} - j\omega\underline{\boldsymbol{\mu}}\bullet\mathbf{H} \\ \nabla\times\mathbf{H} = j\omega\underline{\boldsymbol{\varepsilon}}\bullet\mathbf{E} + j\omega\underline{\boldsymbol{\sigma}}\bullet\mathbf{H} \end{cases}$$

where we used the EH (Tellegen) representation of the constitutive relations [17]. Under time harmonic excitations, the generic entry of the four constitutive tensors is, in general, a complex quantity.

We, first, adopt a cylindrical coordinate system and decompose the electromagnetic field vectors in their longitudinal and transverse components with respect to $\hat{\mathbf{r}}$–direction:

$$\begin{cases} \mathbf{E} = \mathbf{E}_t + E_r\hat{\mathbf{r}} \\ \mathbf{H} = \mathbf{H}_t + H_r\hat{\mathbf{r}} \end{cases} \quad \text{with} \quad \begin{cases} \mathbf{E}_t = E_\varphi\hat{\boldsymbol{\varphi}} + E_z\hat{\mathbf{z}} \\ \mathbf{H}_t = H_\varphi\hat{\boldsymbol{\varphi}} + H_z\hat{\mathbf{z}} \end{cases}.$$

In this geometry the generic component of the electric and magnetic fields can be given by:

$$\Psi(r,\varphi,z) = \frac{1}{2\pi}\sum_{n=-\infty}^{+\infty} e^{-jn\varphi}\int_{-\infty}^{+\infty}\tilde{\Psi}(r,\varphi,\beta)e^{-j\beta z}d\beta$$

being $\tilde{\Psi}$ the generic component of the electric and magnetic fields in the Fourier domain. So, by applying the Fourier transform we can substitute $\partial/\partial z \to j\beta$, and $\partial/\partial\varphi \to jn$.

After some algebraic manipulations, we can write:

1. Two linear relations among the longitudinal and the transverse components of the spectral electromagnetic field with respect to the radial axis:

$$\tilde{E}_r = \frac{1}{\omega r(\varepsilon_{rr}\mu_{rr} - \sigma_{rr}\tau_{rr})}\cdot \left\{\begin{array}{l} [\omega r(\sigma_{rr}\tau_{rz} - \varepsilon_{rz}\mu_{rr}) + n\sigma_{rr}]\tilde{E}_z + \\ -[\beta\sigma_{rr} - \omega(\tau_{r\varphi}\sigma_{rr} - \mu_{rr}\varepsilon_{r\varphi})]\tilde{E}_\varphi + \\ +[\omega r(\mu_{rz}\sigma_{rr} - \mu_{rr}\sigma_{rz}) + n\mu_{rr}]\tilde{H}_z + \\ -[\beta\mu_{rr} - \omega(\mu_{r\varphi}\sigma_{rr} - \mu_{rr}\sigma_{r\varphi})]\tilde{H}_\varphi \end{array}\right\} \quad (1)$$

$$\tilde{H}_r = \frac{1}{\omega r(\varepsilon_{rr}\mu_{rr} - \sigma_{rr}\tau_{rr})}\cdot \left\{\begin{array}{l} [\omega r(\varepsilon_{rz}\tau_{rr} - \varepsilon_{rr}\tau_{rz}) - n\varepsilon_{rr}]\tilde{E}_z + \\ +[\beta\varepsilon_{rr} - \omega(\tau_{r\varphi}\varepsilon_{rr} - \tau_{rr}\varepsilon_{r\varphi})]\tilde{E}_\varphi + \\ -[\omega(\mu_{rz}\varepsilon_{rr} - \tau_{rr}\sigma_{rz}) + n\tau_{rr}]\tilde{H}_z + \\ +[\beta\tau_{rr} + \omega(\tau_{rr}\sigma_{r\varphi} - \mu_{r\varphi}\varepsilon_{rr})]\tilde{H}_\varphi \end{array}\right\} \quad (2)$$

2. The subsystem of differential equations describing the transverse components of the electromagnetic field:

$$\begin{cases} \dfrac{d}{dr}\mathbf{V} = -\underline{\mathbf{C}}_{VI}\cdot\mathbf{I} - \underline{\mathbf{C}}_{VV}\cdot\mathbf{V} \\ \dfrac{d}{dr}\mathbf{I} = -\underline{\mathbf{C}}_{II}\cdot\mathbf{I} - \underline{\mathbf{C}}_{IV}\cdot\mathbf{V} \end{cases} \quad (3)$$

with: $\begin{cases} \mathbf{V} = \tilde{\mathbf{E}}_t \\ \mathbf{I} = \tilde{\mathbf{H}}_t \end{cases}$ and $\mathbf{I} = \tilde{\mathbf{H}}_t$.

2.2 Bianisotropic layer

It can be verified that the matrices $\underline{\mathbf{C}}_{VI}$, $\underline{\mathbf{C}}_{IV}$, $\underline{\mathbf{C}}_{VV}$, and $\underline{\mathbf{C}}_{II}$ satisfy the following symmetry (duality) relations:

$$\begin{cases} \underline{\mathbf{C}}_{VI}(\underline{\boldsymbol{\varepsilon}},\underline{\boldsymbol{\mu}},\underline{\boldsymbol{\sigma}},\underline{\boldsymbol{\tau}}) = \underline{\mathbf{C}}_{VV}(\underline{\boldsymbol{\tau}},\underline{\boldsymbol{\sigma}},\underline{\boldsymbol{\mu}},\underline{\boldsymbol{\varepsilon}}) \\ \underline{\mathbf{C}}_{II}(\underline{\boldsymbol{\varepsilon}},\underline{\boldsymbol{\mu}},\underline{\boldsymbol{\sigma}},\underline{\boldsymbol{\tau}}) = \underline{\mathbf{C}}_{VV}(\underline{\boldsymbol{\mu}},\underline{\boldsymbol{\varepsilon}},-\underline{\boldsymbol{\sigma}},-\underline{\boldsymbol{\tau}}) \\ \underline{\mathbf{C}}_{IV}(\underline{\boldsymbol{\varepsilon}},\underline{\boldsymbol{\mu}},\underline{\boldsymbol{\sigma}},\underline{\boldsymbol{\tau}}) = -\underline{\mathbf{C}}_{VI}(\underline{\boldsymbol{\mu}},\underline{\boldsymbol{\varepsilon}},-\underline{\boldsymbol{\sigma}},-\underline{\boldsymbol{\tau}}) \end{cases} \quad (4)$$

which greatly add to the simplicity of the final expressions.

In this very general case, the evaluation of the elements of the 2×2 matrix $\underline{\mathbf{C}}_{VV}$ is quite cumbersome. We found that they are given by:

$$C_{13} = \frac{j}{\omega r(\varepsilon_{rr}\mu_{rr} - \sigma_{rr}\tau_{rr})}\cdot \left\{\begin{array}{l} \omega r[\beta(\mu_{rr}\varepsilon_{rz} - \tau_{rz}\sigma_{rr}) + \omega[\mu_{\varphi r}(\varepsilon_{rz}\tau_{rr} - \varepsilon_{rr}\tau_{rz}) + \\ -\tau_{\varphi r}(\varepsilon_{rz}\mu_{rr} - \sigma_{rr}\tau_{rz}) + \tau_{\varphi z}(\varepsilon_{rr}\mu_{rr} - \sigma_{rr}\tau_{rr})]] + \\ n[\beta\sigma_{rr} - \omega(\varepsilon_{rr}\mu_{\varphi r} - \sigma_{rr}\tau_{\varphi r})] \end{array}\right\}$$

$$C_{14} = \frac{j}{\omega(\varepsilon_{rr}\mu_{rr} - \sigma_{rr}\tau_{rr})}\cdot \left\{\begin{array}{l} \beta^2\sigma_{rr} + \beta\omega[\mu_{\varphi r}\varepsilon_{rr} - \varepsilon_{r\varphi}\mu_{rr} + \sigma_{rr}(\tau_{r\varphi} - \tau_{\varphi r}) \\ +\omega^2[\tau_{\varphi r}(\varepsilon_{r\varphi}\mu_{rr} - \sigma_{rr}\tau_{r\varphi}) - \tau_{\varphi\varphi}(\varepsilon_{rr}\mu_{rr} - \sigma_{rr}\tau_{rr}) + \\ -\mu_{\varphi r}(\varepsilon_{r\varphi}\tau_{rr} - \varepsilon_{rr}\tau_{r\varphi})] \end{array}\right\}$$

$$C_{23}=\frac{-j}{\omega r(\varepsilon_{rr}\mu_{rr}-\sigma_{rr}\tau_{rr})}\cdot \cdot\begin{Bmatrix}\omega^2 r^2[\tau_{zz}(\varepsilon_{rr}\mu_{rr}-\sigma_{rr}\tau_{rr})+\mu_{zr}(\varepsilon_{rz}\tau_{rr}-\mu_{rr}\sigma_{rz})+\\ -\tau_{zr}(\mu_{rr}\varepsilon_{rz}-\tau_{rz}\sigma_{rr})]+\\ \omega rn[\varepsilon_{r\varphi}\mu_{rr}-\varepsilon_{rr}\mu_{z\varphi}+\sigma_{rr}(\tau_{z\varphi}-\tau_{rz})+n^2\sigma_{rr}]\end{Bmatrix}$$

$$C_{24}=\frac{-j}{\omega r(\varepsilon_{rr}\mu_{rr}-\sigma_{rr}\tau_{rr})}\cdot \cdot\begin{Bmatrix}\omega r[\beta(\varepsilon_{rr}\mu_{z\varphi}-\tau_{zr}\sigma_{rr})+\omega[\mu_{zr}(\varepsilon_{r\varphi}\tau_{rr}-\varepsilon_{rr}\tau_{r\varphi})+\\ +\tau_{z\varphi}(\varepsilon_{rr}\mu_{rr}-\sigma_{rr}\tau_{rr})-\tau_{zr}(\varepsilon_{r\varphi}\mu_{rr}-\sigma_{rr}\tau_{r\varphi})]]+\\ n[\beta\sigma_{rr}+\omega(\varepsilon_{r\varphi}\mu_{rr}-\sigma_{rr}\tau_{r\varphi})]\end{Bmatrix}$$

Equation (3) represents a first order system of coupled differential equations in the radial coordinate r. If the coefficients were independent of r, its solution could formally be written in terms of an infinite set of eigenmodes, each obeying a r-dependence: $e^{\lambda r}$, with λ being an eigenvalue of

$$\underline{\mathbf{C}}=\begin{pmatrix}\underline{\mathbf{C}}_{VI} & \underline{\mathbf{C}}_{VV}\\ \underline{\mathbf{C}}_{II} & \underline{\mathbf{C}}_{II}\end{pmatrix}.$$

In the layered structure with cylindrical symmetry under examination, even for constant material parameters with respect to r, $\underline{\mathbf{C}}$ depends on r via several terms. In the special case of isotropic cylindrical structures, 1/r this leads to the well known eigenmodes expressed in terms of Hankel functions. In the general bianisotropic case, we can combine the four equations (ELT) and obtain a wave equation with non constant coefficients for each of the four transverse components of the electric and magnetic field.

System (3) can be decoupled when:

$$\begin{cases}\underline{\mathbf{C}}_{VV}=0\\ \underline{\mathbf{C}}_{II}=0\end{cases}. \tag{5}$$

Let us now consider a bianisotropic medium which, adopting the classification in [18], falls in the second class of the magnetic group of the third category:

$$\underline{\boldsymbol{\varepsilon}}=\begin{pmatrix}\varepsilon_{rr}&0&0\\0&\varepsilon_{\varphi\varphi}&0\\0&0&\varepsilon_{zz}\end{pmatrix},\ \underline{\boldsymbol{\mu}}=\begin{pmatrix}\mu_{rr}&0&0\\0&\mu_{\varphi\varphi}&0\\0&0&\mu_{zz}\end{pmatrix},$$
$$\underline{\boldsymbol{\sigma}}=\begin{pmatrix}0&\sigma_{r\varphi}&0\\\sigma_{\varphi r}&0&0\\0&0&0\end{pmatrix},\ \underline{\boldsymbol{\tau}}=\begin{pmatrix}0&\tau_{r\varphi}&0\\\tau_{\varphi r}&0&0\\0&0&0\end{pmatrix} \tag{6}$$

A typical example of medium described by constitutive tensors of the second class of the magnetic group of the third category is the Ω medium [15].

When (6) holds, the subsystem of differential equations describing the transverse components of the electromagnetic field can be completely described in terms of the elements of the matrix $\underline{\mathbf{C}}_{VI}$:

$$\underline{\mathbf{C}}_{VI}=\frac{n}{j\omega\varepsilon_{rr}r}\bullet \bullet\begin{pmatrix}-(\beta+\omega\tau_{\varphi r}) & \dfrac{\beta^2+\beta(\sigma_{r\varphi}+\tau_{\varphi r})\omega+(\sigma_{r\varphi}\tau_{\varphi r}-\varepsilon_{rr}\mu_{\varphi\varphi})\omega^2}{n}\\ -\dfrac{n^2-\omega^2r^2\varepsilon_{rr}\mu_{zz}}{n} & \beta+\omega\sigma_{r\varphi}\end{pmatrix} \tag{7}$$

The wave equations satisfied by $\tilde{E}_z$ and $\tilde{H}_z$ are given in terms of the constitutive parameters:

$$\begin{cases}\dfrac{\partial^2\tilde{E}_z}{\partial r^2}+\dfrac{1}{r}\dfrac{\partial\tilde{E}_z}{\partial r}+\dfrac{\tilde{E}_z}{r^2\varepsilon_{\varphi\varphi}}\cdot \cdot\begin{bmatrix}r^2\varepsilon_{zz}[-\beta^2+\beta\omega(\tau_{r\varphi}-\sigma_{r\varphi})+\omega^2(\mu_{rr}\varepsilon_{\varphi\varphi}+\sigma_{r\varphi}\tau_{r\varphi})]+\\ -n^2\varepsilon_{\varphi\varphi}\end{bmatrix}=0\\ \dfrac{\partial^2\tilde{H}_z}{\partial r^2}+\dfrac{1}{r}\dfrac{\partial\tilde{H}_z}{\partial r}+\dfrac{\tilde{E}_z}{r^2\mu_{\varphi\varphi}}\cdot \cdot\begin{bmatrix}r^2\varepsilon_{zz}[-\beta^2+\beta\omega(\tau_{r\varphi}-\sigma_{r\varphi})+\omega^2(\mu_{rr}\varepsilon_{\varphi\varphi}+\sigma_{r\varphi}\tau_{r\varphi})]+\\ -n^2\mu_{rr}\end{bmatrix}=0\end{cases} \tag{8}$$

The wave equations are Kummer differential equations [19] which can be solved in a closed analytical form in terms of the Bessel function of the first and second kind: $J_n(\cdot)$ and $Y_n(\cdot)$.

$$\begin{cases}\tilde{E}_z=\begin{cases}C_1J_n\left(-jr\sqrt{\dfrac{\varepsilon_{zz}}{\varepsilon_{\varphi\varphi}}}\sqrt{\beta^2+\beta\omega(\sigma_{\varphi r}-\tau_{r\varphi})-\omega^2(\mu_{rr}\varepsilon_{\varphi\varphi}+\sigma_{\varphi r}\tau_{r\varphi})}\right)+\\ +C_2Y_n\left(-jr\sqrt{\dfrac{\varepsilon_{zz}}{\varepsilon_{\varphi\varphi}}}\sqrt{\beta^2+\beta\omega(\sigma_{\varphi r}-\tau_{r\varphi})-\omega^2(\mu_{rr}\varepsilon_{\varphi\varphi}+\sigma_{\varphi r}\tau_{r\varphi})}\right)\end{cases}\\ \tilde{H}_z=\begin{cases}C_1J_n\left(-jr\sqrt{\dfrac{\mu_{zz}}{\mu_{rr}}}\sqrt{\beta^2+\beta\omega(\sigma_{r\varphi}-\tau_{\varphi r})-\omega^2(\mu_{\varphi\varphi}\varepsilon_{rr}+\sigma_{r\varphi}\tau_{\varphi r})}\right)+\\ +C_2Y_n\left(-jr\sqrt{\dfrac{\mu_{zz}}{\mu_{rr}}}\sqrt{\beta^2+\beta\omega(\sigma_{r\varphi}-\tau_{\varphi r})-\omega^2(\mu_{\varphi\varphi}\varepsilon_{rr}+\sigma_{r\varphi}\tau_{\varphi r})}\right)\end{cases}\end{cases} \tag{9}$$

3. Shielding Effectiveness of a Bianisotropic Cylindrical Grounded Slab

Let us, now, consider the case, which might be interested for practical applications. It comprises cylindrical grounded layers filled with bianisotropic and/or inhomogeneous media in presence of a homogeneous isotropic half-space (see Fig.1)

Let us first denote with:

1. $F^E_{1,2}$, $G^E_{1,2}$ the solutions of the wave equations for $\tilde{E}_z$ in the grounded slab (denoted with the subscript $_{(1)}$) and in the homogeneous isotropic half-space (denoted with the subscript $_{(2)}$), respectively,
2. $F^H_{1,2}$, $G^H_{1,2}$ the solutions of the wave equations for $\tilde{H}_z$ in the grounded slab and in the homogeneous isotropic half-space, respectively.

These solutions can be found in a closed analytical form or in terms of interpolating functions.

When a plane wave (no current source) impinges on the grounded slab of height d, the electromagnetic field may be represented in terms of a single spectral component as: $E_{inc}(x, y, z) = E_{in} \exp[j(k_x x + k_z z)]$, where

$$\begin{cases} k_x = k_0 \sin(\theta_{inc}) \cos(\varphi_{inc}) \\ k_z = k_0 \cos(\theta_{inc}) \end{cases} \text{ and } (\theta_{inc}, \varphi_{inc})$$

define the angle of incidence. In this case we are able to derive the exact expression for the shielding effectiveness defined as the ratio of the total electric field that is incident on the boundary and the electric field that is transmitted through the boundary for TE(**r**) and TM(**r**) waves:

$$SE = 20 \log_{10} \left| \frac{E_{inc}}{E_{tr}} \right| \tag{10}$$

For TE(**r**) waves the shielding effectiveness is given by:

$$SE^{TE} = \\ = 20 \log_{10} \left| r_0 Z_0^{TE} \frac{A^{TE} D^{TE} - B^{TE} C^{TE}}{S^{TE}(r_0)[B^{TE} + r_0 Z_0^{TE} A^{TE} D^{TE}] + r_0 S'^{TE}(r_0) B^{TE}} \right| \tag{11}$$

For TM(**r**) waves the shielding effectiveness is given by:

$$SE^{TM} = [S^{TM}(r_0) + r_0 S'^{TM}(r_0)] \\ 20 \log_{10} \left| \frac{A^{TM} D^{TM} - B^{TM} C^{TM}}{S^{TM}(r_0)[A^{TM} + r_0 Y_0^{TM} C^{TM}] + r_0 S'^{TM}(r_0) A^{TM}} \right| \tag{12}$$

where we have:

- $\begin{cases} Z_0^{TE} = j\omega\mu_0\mu_r \\ Y_0^{TM} = j\omega\varepsilon_0\varepsilon_r \end{cases}$,
- $Y_0^{TM} = j\omega\varepsilon_0\varepsilon_r$
- $E_{inc} = V_0 S^{TE}$ for the TE(**r**) waves and
- $E_{inc} = V_0 S^{TM}$ for the TM(**r**) waves,
- $$\begin{cases} A^{TE} = \dfrac{1}{r_0} \dfrac{G^E(r_0 + d) P_E^F(r_0) - F^E(r_0 + d) P_E^G(r_0)}{T_E^{(1,1)}} \\ B^{TE} = -C_{12}(r_0) \dfrac{V_E^{(1,2)}}{T_E^{(1,1)}} \\ C^{TE} = \dfrac{1}{r_0} \dfrac{1}{r_0 + d} \dfrac{P_E^F(r_0 + d) P_E^G(r_0) - P_E^F(r_0) P_E^G(r_0 + d)}{C_{12}(r_0 + d) T_E^{(1,1)}} \\ D^{TE} = \dfrac{1}{r_0 + d} \dfrac{C_{12}(r_0)}{C_{12}(r_0 + d)} \cdot \\ \quad \cdot \dfrac{G^E(r_0) P_E^F(r_0 + d) - F^E(r_0) P_E^G(r_0 + d)}{T_E^{(1,1)}} \end{cases}$$
- $$\begin{cases} A^{TM} = \dfrac{1}{r_0 + d} \dfrac{C_{34}(r_0)}{Y_{TM}(r_0 + d)} \cdot \\ \quad \cdot \dfrac{G^H(r_0) P_H^F(r_0 + d) - F^H(r_0) P_H^G(r_0 + d)}{T_H^{(1,1)}} \\ B^{TM} = \dfrac{1}{r_0} \dfrac{1}{r_0 + d} \cdot \\ \quad \cdot \dfrac{P_H^G(r_0) P_H^F(r_0 + d) - P_H^G(r_0 + d) P_H^F(r_0)}{T_H^{(1,1)}} \\ C^{TM} = -C_{34}(r_0) \dfrac{V_H^{(1,2)}}{T_H^{(1,1)}} \\ D^{TM} = \dfrac{1}{r_0} \dfrac{G^H(r_0 + d) P_H^F(r_0) - F^H(r_0 + d) P_H^G(r_0)}{T_H^{(1,1)}} \end{cases}$$
- $P_A^B(\rho) = B^A(\rho) + \rho B^{A'}(\rho)$

The maximum of the shielding effectiveness is obtained when the following relations hold:

$$\begin{cases} \dfrac{1}{r_0} + \dfrac{Y_0^{TM} C^{TM}}{A^{TM}} = -\dfrac{S^{TM}(r_0)}{S'^{TM}(r_0)} \\ \dfrac{1}{r_0} + \dfrac{Z_0^{TE} A^{TE} D^{TE}}{B^{TE}} = -\dfrac{S^{TE}(r_0)}{S'^{TE}(r_0)} \end{cases} \tag{13}$$

On the contrary, considering arbitrary sources, integration over all possible spatial frequencies has to be performed to get the electromagnetic fields behind the shields:

$$E_s(x, y, z) = \int_0^{2\pi} \int_0^{+\infty} E_{inc}(\xi, \delta) e^{j\xi[x \sin\delta + z \cos\delta]} \xi d\xi d\delta \tag{14}$$

The inverse Fourier transform of the scattered electric field (14) has to be computed numerically. In far zone for $r \cdot d$, however it can be evaluated in a closed analytical form by applying the equivalence theorem on the interface [20].

4. Numerical Results

In this section some examples of the scattering, radiation and shielding features of the integrated structure with or without metallic patches are shown for different values of the electromagnetic parameters under both vertical and planar excitation conditions. Some experimental results are also presented for comparison.

A microstrip patch antenna excited with the patch current directed primarily in the r direction is studied first and located at (φ_p, z_p) (Fig.1). Because the radius of the excitation probe is usually a very small fraction of the operating wavelength, the probe feed can be approximately treated as a line source with a current density written as:

$$\mathbf{J}(\mathbf{r}) = I_0 \hat{\mathbf{r}} \frac{\delta(\varphi' - \varphi_p) \delta(z' - z_p)}{r}$$

Solving the unknown patch surface current excited through probe feed, the boundary condition that the total electric field tangential to the patch surface must be zero is applied.

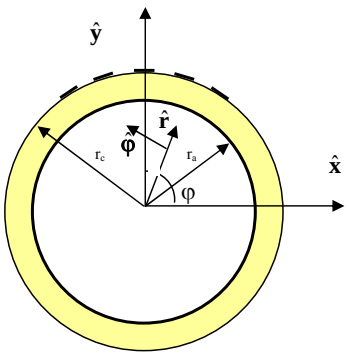

Fig. 1. Geometry of the problem.

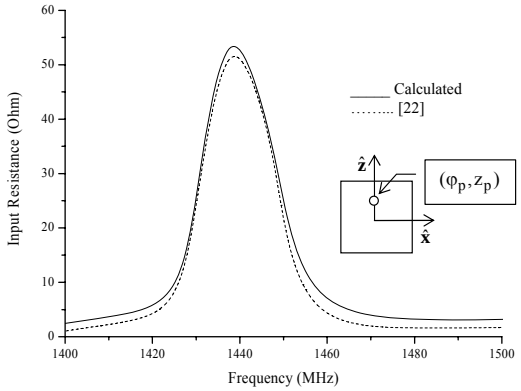

Fig. 2a. Input resistance versus frequency, $\varepsilon_r = 2.98$, $r_c = 8.0762$ cm, $r_a = 8$ cm, $d_\varphi = 4$ cm, $d_z = 6$ cm, $(\varphi_p, z_p) = (90°, 0.81$ cm).

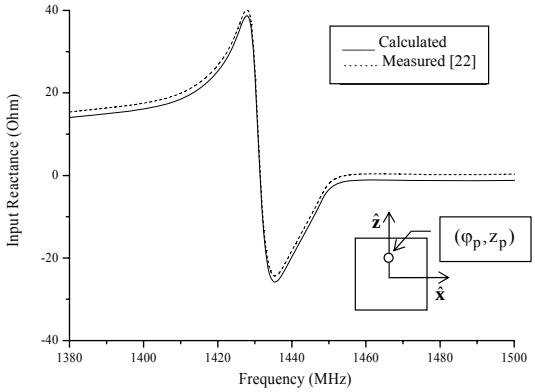

Fig. 2b. Input reactance versus frequency, $\varepsilon_r = 2.98$, $r_c = 8.0762$ cm, $r_a = 8$ cm, $d_\varphi = 4$ cm, $d_z = 6$ cm, $(\varphi_p, z_p) = (90°, 0.81$ cm).

The integral equation is solved by applying Galerkin moment method and using the cavity mode functions, which satisfy the edge singularity as the basis functions [21]. To test the numerical convergence of the results calculated, 12 basis functions are required to obtain good convergent solutions of the input impedance. Excellent agreement between the results calculated and measured [22, 23] is shown in Fig.2. The resonant frequencies, determined from the zero crossing of the reactance curve, are found to be only very slightly affected by curvature variations. It is also shown that the resonant input resistance decreases when the cylinder radius decreases.

The method has also been checked by reproducing results for special cases of non isotropic media from [24] (rectangular microstrip patch antenna over a cylindrical layer filled with a chiral material) and [25] (cylindrical structure filled with a lossless bianisotropic material) that yielded very good agreements.

Fig. 3 shows a very good agreement with the numerical results in [24], where antenna–radiated power patterns of a rectangular microstrip patch antenna over a cylindrical layer filled with a chiral material are presented. A three layered model is assumed, where the relative permittivity ε_r of the substrate is 2.57, the radius a of the conducting core-cylinder is 2.5 cm, the thickness h of the chiral coating cylindrical layer is $0.012\ \lambda_0$ with λ_0 the free-space wavelength. The cylindrical-rectangular microstrip antenna has a dimension of $2\ d_z = d_\varphi = 4.02$ cm. The rectangular patch is fed by a microstrip line parallel to the cylinder axis and connected to the center from its lower side. The length of the feeding line L_f is chosen as a multiple of $\lambda/2$, where λ is the guided wavelength along the line.

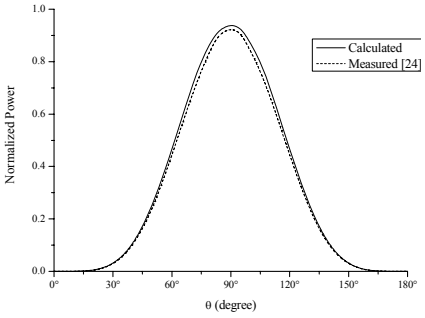

Fig. 3. Normalized power versus a polar angle θ at a fixed azimuth angle $\varphi = 0°$, $\xi_c = 0.005$, $\varepsilon_r = 2.57$, $d_\varphi = 2d_z = 4.02$ cm, $r_a = 2.5$ cm, $r_c = r_a + 0.012\ \lambda_0$, $L_f = \lambda/2$.

Fig.4 shows a very good agreement with the numerical results in [25], where the radiation pattern of an axial Hertzian dipole at $\varphi = z = 0$ in a bianisotropic cylindrical structure is presented. The lossless bianisotropic material is characterized by the constitutive tensors

$$\underline{\boldsymbol{\tau}} = \underline{\boldsymbol{\sigma}} = c_0^{-1} \begin{pmatrix} 0 & \tau_1 & 0 \\ \tau_1 & 0 & 0 \\ 0 & 0 & 0 \end{pmatrix}.$$

In Fig.5 we plot the return loss of probe fed patch antennas loaded by different bianisotropic materials. The main results are the reduction of the resonance frequency when the bianisotropic effect increases and a rotation of the main lobe direction of about five degrees. This result may be attributable to a pair of weakly attenuated, coupled leaky waves which propagate in the bianisotropic medium after their excitation. The radiation patterns, by changing the bianisotropy in a certain range, are very close to each others. Due to this fact, the dominant effect of the bianisotropic material is the reduction of the resonance frequency and, therefore, we can think of designing a microstrip antenna with smaller layout dimensions.

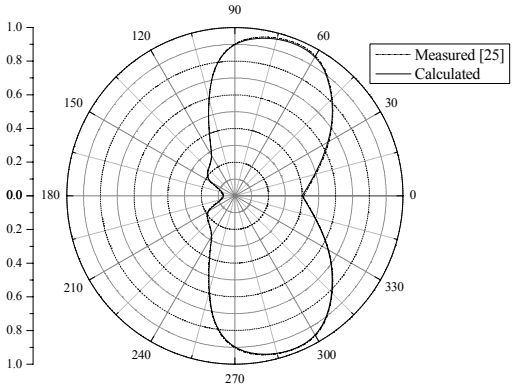

Fig. 4. Radiation pattern for an infinitesimal current at a fixed azimuth angle $\varphi = 0°$, f = 3 GHz, $r_a = 5$ cm, $r_c = 5.1$ cm, $\tau_1 = = 1.3j$.

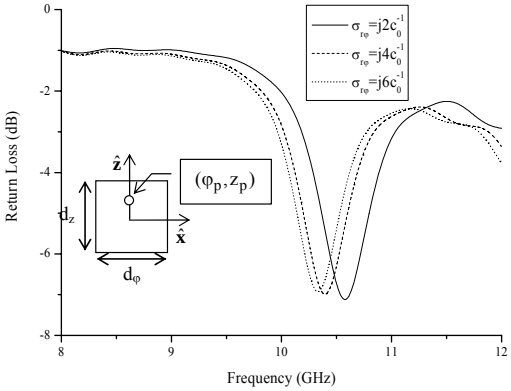

Fig. 5. Return loss versus frequency, $d_\varphi = 1.2$ cm, $d_z = 1.6$ cm, $r_a = 8$ cm, $r_c = 8.08$ cm, $(\varphi_p, z_p) = (90°, 0.45$ cm), $\varepsilon_{rr} = \varepsilon_{zz} = \varepsilon_0$, $\varepsilon_{\varphi\varphi} = 2.2\ \varepsilon_0$, $\mu_{rr} = \mu_{\varphi\varphi} = \mu_{zz} = \mu_0$, $\sigma_{\varphi r} = \tau_{\varphi r} = j\ 10\ c_0^{-1}$, $c_0^{-1} = = (\mu_0\ \varepsilon_0)^{1/2}$.

5. Conclusions

In this paper we have presented a derivation of the equivalent two-port circuit representation along the stratification axis for bianisotropic cylindrical layered structures. We have proposed also an analytical study of the shielding effectiveness of both bianisotropic materials located in multilayered configuration deducing the expression of the shielded fields sustained both by plane wave and arbitrary sources in a closed analytical form. Numerical results have been, also, presented showing the effects of the electromagnetic parameters on the field quantities of the integrated structure.

6.Acknowledgements

The authors would like to thank an anonymous reviewer for his/her useful comments that have helped to improve the quality of the manuscript.

References

[1] SERDYUKOV, A., SEMCHENKO, I., TRETYAKOV, S., SIHVOLA, A. *Electromagnetics of Bi-Anisotropic Materials: Theory and Applications*. Amsterdam: Gordon and Breach Science Publishers, p. 37-41, 2001.

[2] TAN, E. L., TAN, S.Y. Spectral-domain dyadic Green's functions for surface current excitation in planar stratified bianisotropic media. *IEE Proceedings Microwaves, Antennas and Propagation*. 1999, vol. 146, p. 394 -400.

[3] VEGNI, L., ALÚ, A., BILOTTI, F. Electromagnetic field solution in curved structures with local bianisotropic loading media. In: ZOUHDI, S., SIHVOLA, A., ARSALANE, M. *Advances in Electromagnetics of Complex Media and Metamaterials*, Dordrecht: Kluwer Academic Publishers, p. 439-448, 2002.

[4] OZDEMIR, T., VOLAKIS, J. L. Finite element analysis of doubly curved conformal antennas with material overlays. In *IEEE International Symposium of Antennas and Propagation Society*. 1996, vol. 1, p. 134-137.

[5] CHI-WEI WU, KEMPEL, L.C., ROTHWELL, E.J. Radiation by cavity-backed antennas on an elliptic cylinder. In *IEEE International Symposium of Antennas and Propagation Society*. 2001, vol.1, p. 342 to 345.

[6] SVEZHENTSEV, VANDENBOSCH, G. Model for the analysis of microstrip cylindrical antennas: efficient calculation of the necessary Green's functions. In *IEEE International Symposium of Antennas and Propagation Society*, 2001, vol. 2, p. 615-618.

[7] PERSSON, P., JOSEFSSON, L. Calculating the mutual coupling between apertures on convex cylinders using a hybrid UTD-MoM method. In *IEEE International Symposium of Antennas and Propagation Society*. 1999, vol.2, p. 890-893.

[8] COCKRELL, R., PATHAK, P. H. Diffraction theory techniques applied to aperture antennas on finite circular and square ground planes. *IEEE Transactions on Antennas and Propagation*. 1974, vol. 22, p. 443-448.

[9] CHTTERJEE, JIN, J. M., VOLAKIS, J. L. Edge-based finite elements and vector ABC's applied to 3-D scattering. *IEEE Transactions on Antennas and Propagation*. 1993, vol. 41, no. 2, p. 221-226.

[10] VEGNI, L., CICCHETTI, R., CAPECE, P. Spectral dyadic Green's function formulation for planar integrated structures. *IEEE Transactions on Antennas and Propagation*. 1988, vol. 36, p. 1057-1065.

[11] TOSCANO, A., VEGNI, L. Spectral dyadic Green's function formulation for planar integrated structures with a grounded chiral slab. *Journal of Electromagnetic Waves and Applications*. 1992, vol. 6, p. 751-769.

[12] TOSCANO, A., VEGNI, L. Spatial electromagnetic fields in chiral integrated structures via Sommerfeld integrals. *IEICE Transactions on Electronics*. 1995, vol. 10, p. 1391-1401.

[13] TOSCANO, A., VEGNI, L. Electromagnetic field computation in planar integrated structure with a biaxial grounded slab. *IEEE Transactions on Magnetics*. 1993, vol. 29, p. 1726-1729.

[14] TOSCANO, A., VEGNI, L. Spectral electromagnetic modeling of a planar integrated structure with a general grounded anisotropic slab. *IEEE Transactions on Antennas and Propagation*. 1993, vol. 41, p. 362-370.

[15] TOSCANO, A., VEGNI, L. Electromagnetic waves in planar integrated pseudochiral Ω structures. In *Progress in Electromagnetic Research*. 1994, vol. 9, p.181-216.

[16] VEGNI, L., TOSCANO, A., BILOTTI, F. Shielding and radiation characteristics of planar layered inhomogeneous composites. *IEEE Transactions on Antennas and Propagation*. 2003, vol. 51, p. 2869 to 2877.

[17] KONG, J. A. *Electromagnetic Wave Theory*. New York: Wiley, 2nd Ed., 1990.

[18] DIMITRIEV, V. Complete tables of the second rank constitutive tensors for linear homogeneous bianisotropic media described by the

point magnetic groups of symmetry and some general properties of the media. In *Microwave and Optoelectronics Conference*, SBMO/ IEEE MTT-S. 1999, vol. 2, p. 435-439.

[19] GOLDSTEIN *Advanced Methods for Differential Equations*. NASA SP-316, Washington, DC: U.S. Government Printing Office, 1973.

[20] POPOVSKI, B., TOSCANO, A., VEGNI, L. Radial and asymptotic closed form representation of the spatial microstrip dyadic Green's function. *Journal of Electromagnetic Waves and Applications*. 1995, vol. 9, p. 97-126.

[21] MOSIG, J. R. Integral equation techniques. In *Numerical Techniques for Microwave and Millimeter-Waves Passive Structures*, T. Itoh, Ed. New York, NY: Wiley, 1989, ch. 3, p. 133-213.B.

[22] WONG, K. L., CHENG, Y. T., ROW, J. S. Analysis of a cylindrical-rectangular microstrip structure with an air gap. *IEEE Transactions on Microwave Theory and Techniques*. 1994, vol. 42, p. 1032-1037.

[23] WONG, K. L., WANG, S. M., KE, S. Y. Measured input impedance and mutual coupling of rectangular microstrip antennas on a cylindrical surface. Microwave and Optical Technology Letters. 1996, vol. 11, p. 49-50.

[24] LI, W., ZHAO, X. A spatial-domain method of moments analysis of a cylindrical-rectangular chirostrip. In *Progress In Electromagnetics Research*, PIERS 35, p. 165-182, 2002.

[25] YOON, J. H., LEE, S. M., AU, G. C., LEE, H. C. Cylindrical vector wave function representation of Green's dyadics for uniaxial bianisotropic media. *TENCON 99, Proceedings of the IEEE Region 10 Conference*, p. 522-525, 1999.

About Authors...

Lucio VEGNI was born in Castiglion Fiorentino, Italy, on June 20, 1943. He received the degree in electronic engineering from the University of Rome, Rome, Italy. Since 1992, he has been with the University of "Roma Tre," Rome, Italy, where he is currently a Full Professor of electromagnetic field theory. His research interests are in the areas of microwave- and millimeter-wave circuits and antennas with particular emphasis to the EMC problems. Prof. Vegni is a member of the European chiral group and the Italian Electrical and Electronic Society (AEI).

Alessandro TOSCANO was born in Capua, Italy, on June 26, 1964. He received the degree in electronic engineering and the Ph.D. degree from the University of Rome "La Sapienza," Rome, Italy, in 1988 and 1993, respectively. In 1993, he joined the Department of Electronic Engineering, University of "Roma Tre," Rome, where he is currently an Associate Professor. His research interests are in the areas of microwave and millimeter-wave circuits and antennas including dyadic Green functions, homogeneous and inhomogeneous bi-anisotropic media, wave propagation, scattering, and general techniques in electromagnetics of complex media.